unmixing of the alloy reaches a steady state from about 3 h ageing time and the volume fraction of precipitates is practically constant with ageing time. However, the increase of ageing time leads to an important decrease in the cobalt concentration of precipitates.

7. Concluding remarks

ASAXS experiments have allowed the kinetic study of coarsening of the binary Cu–2 at.% Co alloy for ageing at 923 K. The cobalt precipitation is controlled by the cobalt diffusion in a copper matrix and a steady state is reached from about 3 h ageing time.

Spherical-precipitate simulation of almost size monodispersion is in good agreement with the experimental data for 3 h ageing time. After 120 h ageing, the size dispersion is more important and comparison between experimental and fitted data is not so good.

Determination of the cobalt concentration of precipitates was carried out with measurements of absolute scattered intensity. This concentration decreases when ageing time increases.

References

ANCRENAZ, P. & SERVANT, C. (1992). *J. Phys. (Paris) I*, **2**, 1113–1128.

ASHCROFT, N. M. & LEKNER, J. (1966). *Phys. Rev.* **145**, 83.

BOUZID, N., SERVANT, C. & LYON, O. (1988). *Philos Mag.* **57**, 343–359.

FONTAINE, D. DE (1979). *Solid State Physics*, Vol. 34, *Configurational Thermodynamics of Solid Solutions*, edited by E. SEITZ & D. H. TURNBULL, pp. 73–274. New York: Academic Press.

GUINIER, A. & FOURNET, G. (1955). *Small-Angle X-ray Scattering*. New York: John Wiley.

HENNION, M., RONZAUD, D. & GUYOT, P. (1982). *Acta Metall.* **30**, 599–610.

LIFSHIFTZ, I. M. & SLYOZOV, V. V. (1961). *J. Phys. Chem. Solids*, **19**, 35.

LYON, O., HOYT, J. J., PRO, D., DAVIS, B. E. C., CLARK, B., DE FONTAINE, D. & SIMON, J. P. (1985). *J. Appl. Cryst.* **18**, 480.

SASAKI, S. (1984). *Anomalous Scattering Factors for Synchrotron Radiation Users, Calculating using Cromer and Libermann Method*, pp. 22–83. National Laboratory for High Energy Physics, Ohomachi, Japan.

Acta Cryst. (1993). B**49**, 463–468

Thermal Effects in the Structure of Ammonium Perrhenate

BY BRIAN M. POWELL

AECL Research, Chalk River Laboratories, Chalk River, Ontario K0J 1J0, Canada

AND R. JULIAN C. BROWN, ANNE M. C. HARNDEN AND J. KIRK REID

Chemistry Department, Queen's University, Kingston, Ontario K7L 3N6, Canada

(*Received* 20 *July* 1992; *accepted* 1 *December* 1992)

Abstract

The structure of ND_4ReO_4 has been determined by neutron powder diffraction at 20 K intervals from 20 to 240 K and at 298 K. At 20 K the N—D bond distance is 1.025 (2) Å, the Re—O bond distance is 1.733 (2) Å and the D···O interionic distance is 1.878 (2) Å. The thermal expansion is normal at low temperatures, but becomes anomalous above about 90 K. The anion orientation changes by 3.2° over the whole temperature range while the cation orientation changes by 28°, and at the higher temperatures the deuterium thermal ellipsoid becomes highly elongated in the direction perpendicular to the N—D bond. This lends support to the pseudo-spin model for the anomalous behaviour of this salt, in which disorder between two non-equivalent orientations of the ammonium ion is assumed.

Introduction

Ammonium perrhenate crystallizes in the scheelite structure (tetragonal, $I4_1/a$) (Kruger & Reynhardt, 1978). It does not undergo any phase transition between helium temperature and about 400 K, but its thermal-expansion behavior is remarkable (Brown, Smeltzer & Heyding, 1976; Segel, Karlsson, Gustavson & Edstrom, 1985). The unit cell expands along the *c* axis, but contracts along the *a* axis, so that the unit-cell volume hardly changes even though the axial expansion coefficients are much larger than in the isostructural potassium perrhenate. There have been several structural studies, by single-crystal X-ray diffraction (Kruger & Reynhardt, 1978) and powder neutron diffraction (Brown, Segel & Dolling, 1980), but a more systematic study is needed because of the large temperature-dependent changes in the

lattice. In particular it is important to try to characterize the motion of the ammonium ion. A preliminary account of this work has been given by Brown, Shortreed, Szabo, Powell & Stuart (1992).

Recently, a theory to account for the various extraordinary properties of NH_4ReO_4 has been proposed. In this theory two possible stable orientations of the ammonium ion are assumed to be associated with the values ± 1 of a pseudo-spin variable (Taylor, 1987, 1989). These two orientations are identified with the axial and equatorial orientations which have been suggested previously as possible stable orientations for the ammonium ion (Brown, Segel & Dolling, 1980). Since the deuterium–oxygen distances in these two orientations are different, the two orientations differ in energy by an amount which depends on the crystal geometry. In Taylor's theory, the energy difference is assumed to be a linear function of the lattice parameters, and the anomalous properties are shown to be the result of cooperative ordering at low temperatures. The purpose of the present experiments is to test this theory directly by following changes in the deuterium position and thermal motion as the temperature is increased. The powder-diffraction pattern was measured at fairly closely spaced temperatures covering the whole temperature range, so that changes in the structure can be followed almost continuously.

Experimental

The sample used was commercial NH_4ReO_4 powder (Aldrich Chemical Co.) which was deuterated by recrystallization three times from D_2O. The sample was loaded into a thin-walled vanadium can 0.75 cm in diameter and mounted in a variable-temperature closed-cycle cryostat. Measurements were taken on the E3 powder diffractometer with a 30-element multi-detector at the NRU reactor, Chalk River. The monochromator was Si(115) and the diffractometer was calibrated by measuring the profile of a powder sample of silicon whose lattice parameter [a = 5.430940 (35) Å] was calibrated at the National Institute of Standards and Technology. Temperatures were measured by silicon diode thermometers and were held constant to within 0.04 K. Data were collected at scattering angles of between 8.0 and 119.95° at intervals of 0.05° and analyzed using a Rietveld program (Wiles & Young, 1981); scattering lengths were taken from Sears (1986). The background was fitted with either a parabolic or cubic polynomial (with no significant difference in the results). No correction for neutron absorption was applied.

The measurements were performed in two separate series. Series I covered the range from 20 to 140 K in 20 K intervals, and Series II covered the range from 140 to 240 K in 20 K intervals, and 298 K. Between the two series, the sample was demounted and remounted, and adjustments were made to the monochromator for other experiments. The neutron wavelength, calibrated as described, was 1.49978 (9) Å for Series I, and 1.49935 (6) Å for Series II. Within each series, the results are highly consistent, but there is an inconsistency between the two series of measurements, which is manifested as a displacement between the graphs of the two sets of data *versus* temperature, and is apparent in the data in Table 1 as a discrepancy at the common temperature of 140 K. The discrepancy is larger than would be expected from the indicated errors in the calibrated wavelengths and in the lattice parameters, and requires further discussion.

Table 1. *Cell dimensions*

These data were obtained from the neutron diffraction profiles assuming neutron wavelengths of 1.49978 (9) Å for Series I and 1.49935 (6) Å for Series II. E.s.d.'s are given in parentheses and are taken from the Rietveld program output. The space group is $I4_1/a$.

T (K)	a (Å)	c (Å)	c/a	V (Å^3)
Series I				
20	5.99746 (10)	12.39267 (29)	2.06632 (6)	445.76 (2)
40	5.99845 (11)	12.39372 (30)	2.06615 (6)	445.94 (2)
60	5.99972 (11)	12.39806 (30)	2.06644 (6)	446.29 (2)
80	6.00073 (11)	12.40666 (32)	2.06752 (6)	446.75 (2)
100	6.00048 (11)	12.42035 (33)	2.06989 (7)	447.20 (2)
120	5.99842 (12)	12.44133 (35)	2.07410 (7)	447.65 (2)
140	5.99340 (13)	12.47348 (38)	2.08120 (8)	448.06 (2)
Series II				
140	5.98566 (9)	12.45922 (26)	2.08151 (5)	446.39 (2)
160	5.97439 (10)	12.50927 (27)	2.09382 (6)	446.50 (2)
180	5.95552 (12)	12.58428 (34)	2.11304 (7)	446.34 (2)
200	5.92905 (14)	12.68260 (39)	2.13906 (8)	445.84 (3)
220	5.90817 (15)	12.76953 (41)	2.16133 (9)	445.74 (3)
240	5.89399 (15)	12.83853 (46)	2.17824 (10)	446.00 (3)
298	5.87679 (17)	12.97820 (50)	2.20838 (11)	448.22 (3)

The ratio of a parameters at 140 K is 1.00129 (3), and the ratio of c parameters is 1.00114 (4). The two data sets could be combined by applying a correction factor equal to the average ratio of 1.00121 (3) to one or other. This is done in Figs. 1 and 2, which show graphs of all published lattice parameter data, with the Series II data presented both as measured (Table 1) and when multiplied by 1.00121. The discrepancy between the two series of data is within the overall scatter of the other measurements.

The origin of the discrepancy cannot lie in the temperature measurements since a temperature error would cause shifts of opposite sign in a and c, contrary to what is observed. It must lie in the setup of the samples and the diffractometer, which was done four times during the calibration and data-collection procedures. The data has been examined to see if one of the two wavelengths is in error, by comparing the present lattice parameters with previous determinations of the lattice parameters of ammonium and potassium perrhenates. No calibration error is evident, and it would be equally valid

to scale the Series I data rather than the Series II data.

Unit-cell data for $KReO_4$ and NH_4ReO_4 at 298 K were determined by Brown, Smeltzer & Heyding (1976) using Guinier–de Wolff X-ray powder patterns with As_2O_3 as an internal standard. Since this is the only study in which an internal standard was used, the results may be taken as the standard against which other data are judged.

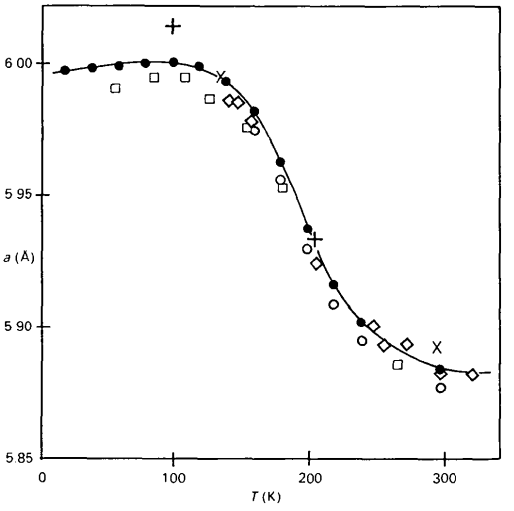

Fig. 1. Lattice parameter *a* in ammonium perrhenate as a function of temperature. The line is a guide to the eye. Legend: ○, present work, series II for 140 K and above, unscaled; ●, present work, series I up to 140 K and series II scaled as described in the text for 140 K and above; □, Segel *et al.* (1985); ◇, Brown *et al.* (1976), of which the point at 298 K was calibrated with an internal standard; +, Brown *et al.* (1980); ×, Kruger & Reynhardt (1978).

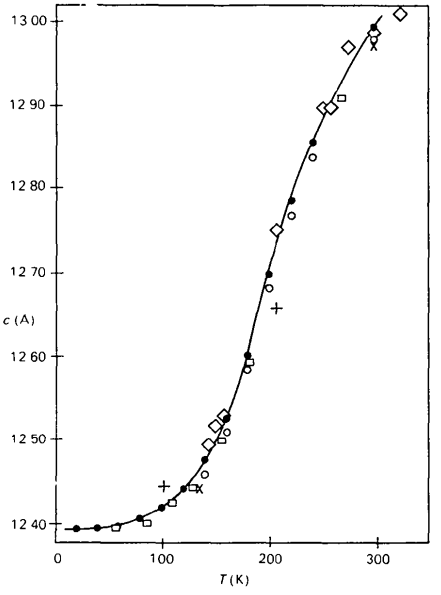

Fig. 2. Lattice parameter *c* in ammonium perrhenate as a function of temperature. Legend is the same as in Fig. 1.

The *a* and *c* parameters of $KReO_4$ determined by Lock & Turner (1975) in a single-crystal X-ray study differ from the standard values by factors of 0.9977 and 0.9975 respectively. The recent neutron diffraction results on $KReO_4$ (Brown, Powell & Stuart, 1993), using the same instrument and the same wavelength calibration as the Series I data reported here, yield lattice parameters which differ from the standard values by factors of 1.0015 and 1.0010, respectively.

For NH_4ReO_4, the lattice parameters determined by Kruger & Reynhardt (1978) in a single-crystal study, after correction from 295 to 298 K, differ from the standard results by factors of 1.019 and 0.9582, respectively. The discrepancies are larger than can be accounted for by a temperature error.

For ND_4ReO_4 the present Series II lattice parameters at 298 K differ from the standard values by factors of 0.99894 and 0.99940, respectively, and multiplication by 1.00121 would bring them into good agreement with the standard results. It should be remembered that the standard data are for NH_4ReO_4 while the neutron diffraction results are for ND_4ReO_4, and there is no reliable report of the change in lattice parameters upon deuteration.

Discussion

The results will be discussed with particular reference to the following aspects: thermal expansion, anion orientation, cation orientation, and cation thermal motion. A projection of part of the unit cell on the **ab** plane is shown in Fig. 3.

All data sets refined satisfactorily using a single deuterium-atom position, *i.e.* a single cation orientation, and led to acceptable anion and cation geometries. The fractional atomic coordinates are given in Table 2, while the anisotropic thermal parameters and structural data are given in Tables 3–7.*

The results confirm that the anomalous thermal expansion begins at about 90 K, and that the *a*-axis contraction and the *c*-axis expansion have their greatest slopes at about 190 K. The onset of anomalous thermal expansion is found at a temperature approximately half of the temperature at the centre of the anomaly, which is consistent with the pseudospin theory (Taylor, 1989).

* Observed and calculated profile data, thermal parameters in real space for deuterium and oxygen, and the diagonalized thermal ellipsoid for deuterium, at each temperature have been deposited with the British Library Document Supply Centre as Supplementary Publication No. SUP 55857 (130 pp.). Copies may be obtained through The Technical Editor, International Union of Crystallography, 5 Abbey Square, Chester CH1 2HU, England.

The anion orientation in the unit cell, defined by the angle β (Fig. 3), changes by 3.25 (19)° between 20 and 298 K. This is considerably more than the corresponding change in $KReO_4$, namely 1.20 (13)°.

The N—D bond length of 1.025 (2) Å taken from the 20 K data (Table 6) is consistent with recent values (1.025–1.030 Å) for an ND_4^+ ion at a site of lower symmetry determined by single-crystal neutron diffraction at helium temperature (Figgis, Kucharski & Forsyth, 1991). The Re—O bond distance and bond angle at 20 K (Table 6) agree well with other published values: 1.737 (5) and 110.3° (Kruger & Reynhardt, 1978), 1.723 (4) Å and 110.8° (Lock & Turner, 1975), and 1.739 (1) Å and 110.5° (Brown, Powell & Stuart, 1993). The discrepancy between values for the Re—O bond distance in the two series of measurements is somewhat larger than the discrepancy in lattice parameters.

The angle α, which specifies the cation orientation in the unit cell (Fig. 3), changes from +18.96 (12)° at 20 K to −10.19 (74)° at 298 K, indicating a major change in the orientation of the ND_4^+ ions. At the lowest temperatures the N—D bonds point (in projection) directly at the axial O atoms, in agreement with the previous neutron-diffraction study (Brown, Segel & Dolling, 1980). As the temperature increases, the deuteron position appears to shift so that the ion rotates about the direction of the *c* axis. In addition, the N—D bond length appears to shorten, and the D—N—D bond angle to get smaller, effects which can be ascribed to increased amplitude of the thermal motion. The $N\cdots O_{ax}$ and $N\cdots O_{eq}$ distances are given in Table 7, and show surprisingly little variation with temperature. The $D\cdots O_{ax}$ and $D\cdots O_{eq}$ distances differ considerably at low temperature, but are approaching equality at room temperature. At 20 K the $D\cdots O_{ax}$ interionic distance is 1.878 (2) Å and the $N—D\cdots O_{ax}$ angle is 161 (1)°.

The thermal amplitudes for N, Re and O increase with temperature as expected. The Re temperature factors are small and apparently negative at low temperatures, similar to the analogous results found in $KReO_4$. This is ascribed to neglect of a correction for absorption (Hewat, 1979; Sears, 1986). The deuterium temperature factor has a large temperature dependence in both the amplitude and orientation of the thermal ellipsoid. With increasing temperature, the thermal ellipsoid reorients so as to remain in a roughly fixed relationship to the N—D bond. The

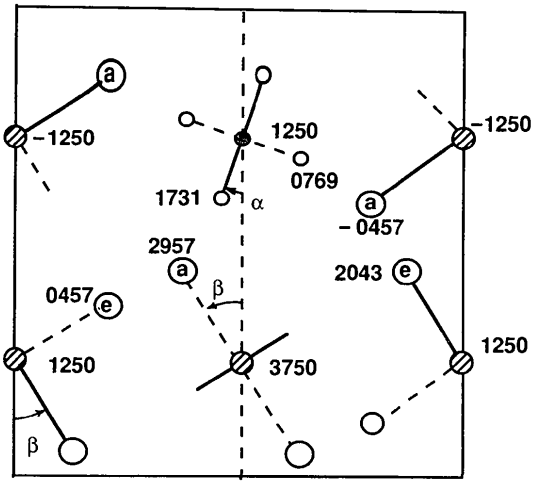

Fig. 3. Projection of part of the unit cell of ND_4ReO_4 on the **ab** plane, showing the surroundings of one ammonium ion. The *z* coordinates (multiplied by 10^4) are shown next to each atom. The ND_4^+ ion (small circles) is in the centre near the top and parts of adjacent ReO_4 ions are shown in large circles. O atoms are labelled '*e*' (equatorial) if bonded to an Re atom with the same *z* as the N atom of the ND_4^+ ion, or '*a*' (axial) if bonded to an Re atom which is displaced by $\pm c/4$. Around each ND_4^+ ion there are four axial and four equatorial O atoms. The angles α and β define the orientation of the cation and anion, respectively, in the unit cell.

Table 2. *Fractional atomic position parameters and R factors*

Parameters are given relative to the origin at $\bar{1}$ and have been multiplied by 10^4. E.s.d.'s are given in parentheses. *N* is at (5000, 7500, 1250) and Re is at (0, 2500, 1250). The expected R_{wp} value was 3.02% for Series I and 2.32% for Series II.

T (K)	R_{wp}	x_D	y_D	z_D	x_O	y_O	z_O
Series I							
20	6.57	4549 (3)	6184 (3)	1731 (1)	2026 (3)	3750 (3)	457 (1)
40	6.67	4554 (3)	6186 (3)	1732 (1)	2025 (3)	3747 (3)	456 (1)
60	6.61	4553 (3)	6187 (3)	1731 (1)	2027 (3)	3746 (3)	457 (1)
80	6.58	4553 (3)	6185 (3)	1730 (1)	2027 (3)	3742 (3)	457 (1)
100	6.55	4556 (3)	6190 (3)	1729 (1)	2029 (3)	3738 (3)	459 (1)
120	6.64	4565 (4)	6186 (3)	1728 (1)	2034 (3)	3729 (3)	457 (1)
140	6.81	4583 (4)	6183 (3)	1721 (2)	2034 (3)	3724 (3)	458 (2)
Series II							
140	4.81	4581 (3)	6196 (2)	1724 (1)	2023 (3)	3714 (2)	460 (1)
160	5.03	4599 (3)	6199 (3)	1721 (1)	2036 (3)	3707 (3)	463 (1)
180	5.36	4640 (4)	6208 (3)	1714 (1)	2054 (3)	3699 (3)	468 (1)
200	5.86	4734 (6)	6218 (4)	1710 (2)	2071 (3)	3680 (4)	471 (2)
220	6.03	4840 (9)	6215 (5)	1695 (2)	2097 (4)	3669 (4)	474 (2)
240	6.00	5033 (13)	6241 (6)	1694 (2)	2116 (4)	3642 (4)	475 (2)
298	5.73	5217 (16)	6293 (7)	1682 (3)	2133 (4)	3621 (5)	487 (2)

Table 3. *Anisotropic thermal parameters for deuterium*

The anisotropic temperature factors are of the form $\exp(-\beta_{11}h^2 - \beta_{22}k^2 - \beta_{33}l^2 - 2\beta_{12}hk - 2\beta_{13}hl - 2\beta_{23}kl)$. The parameters β_{ij} have been multiplied by 10^4, and e.s.d.'s are given in parentheses.

T (K)	β_{11}	β_{22}	β_{33}	β_{12}	β_{13}	β_{23}
Series I						
20	174 (7)	111 (6)	20 (1)	−18 (5)	12 (2)	21 (2)
40	171 (7)	120 (6)	21 (1)	−13 (5)	12 (2)	19 (2)
60	184 (7)	127 (6)	25 (1)	−19 (5)	12 (2)	22 (2)
80	183 (7)	136 (6)	23 (1)	−14 (5)	11 (2)	19 (2)
100	200 (8)	139 (7)	27 (2)	−14 (6)	11 (2)	19 (2)
120	220 (8)	160 (7)	32 (2)	−15 (6)	12 (2)	22 (3)
140	273 (10)	167 (8)	43 (2)	−24 (7)	11 (3)	24 (3)
Series II						
140	266 (7)	162 (6)	39 (1)	−31 (5)	12 (2)	25 (2)
160	338 (9)	188 (6)	46 (2)	−47 (6)	14 (3)	31 (2)
180	502 (13)	218 (8)	54 (2)	−57 (8)	26 (4)	38 (3)
200	847 (20)	281 (10)	60 (3)	−71 (12)	26 (6)	58 (3)
220	1056 (26)	309 (12)	80 (3)	−37 (16)	30 (8)	83 (4)
240	1455 (34)	376 (15)	80 (3)	157 (22)	−28 (10)	85 (4)
298	1703 (44)	568 (20)	101 (4)	332 (29)	−91 (14)	96 (4)

Table 4. *Anisotropic thermal parameters for oxygen*

The anisotropic temperature factors are of the form $\exp(-\beta_{11}h^2 - \beta_{22}k^2 - \beta_{33}l^2 - 2\beta_{12}hk - 2\beta_{13}hl - 2\beta_{23}kl)$. The parameters β_{ij} have been multiplied by 10^4, and e.s.d.'s are given in parentheses.

T (K)	β_{11}	β_{22}	β_{33}	β_{12}	β_{13}	β_{23}
Series I						
20	32 (4)	33 (5)	2 (1)	13 (5)	1 (2)	12 (2)
40	37 (5)	35 (5)	3 (1)	7 (5)	1 (2)	10 (2)
60	45 (5)	45 (5)	5 (1)	14 (5)	2 (2)	8 (2)
80	51 (5)	50 (6)	5 (1)	5 (5)	3 (2)	8 (2)
100	61 (5)	67 (6)	6 (1)	7 (6)	6 (2)	9 (2)
120	78 (6)	79 (7)	7 (1)	−6 (6)	5 (2)	6 (3)
140	94 (7)	96 (7)	12 (2)	−11 (7)	10 (2)	0 (3)
Series II						
140	95 (5)	107 (5)	12 (1)	−27 (5)	20 (2)	3 (2)
160	104 (5)	115 (5)	14 (1)	−28 (6)	23 (2)	8 (2)
180	106 (6)	135 (6)	16 (1)	−25 (6)	26 (2)	6 (2)
200	112 (7)	173 (8)	23 (1)	−22 (7)	40 (3)	−2 (3)
220	133 (9)	208 (9)	25 (2)	−51 (8)	35 (3)	1 (3)
240	155 (10)	213 (9)	34 (2)	−40 (8)	44 (3)	−5 (3)
298	204 (11)	287 (11)	42 (2)	−77 (10)	48 (3)	−3 (3)

Table 5. *Anisotropic thermal parameters for nitrogen and rhenium*

The anisotropic temperature factors are of the form $\exp(-\beta_{11}h^2 - \beta_{22}k^2 - \beta_{33}l^2 - 2\beta_{12}hk - 2\beta_{13}hl - 2\beta_{23}kl)$. The parameters β_{ij} have been multiplied by 10^4, and e.s.d.'s are given in parentheses.

T (K)	β_{11} (N)	β_{33} (N)	β_{11} (Re)	β_{33} (Re)
Series I				
20	61 (4)	1 (2)	−12 (3)	−3 (1)
40	65 (4)	1 (2)	−8 (4)	−2 (1)
60	65 (4)	4 (2)	0 (4)	−1 (1)
80	70 (4)	4 (2)	−6 (4)	4 (1)
100	81 (5)	6 (2)	1 (4)	6 (2)
120	90 (5)	7 (2)	1 (4)	10 (2)
140	101 (5)	13 (2)	11 (5)	12 (2)
Series II				
140	78 (4)	11 (2)	32 (3)	0 (1)
160	90 (4)	13 (2)	43 (4)	5 (1)
180	113 (5)	12 (2)	38 (4)	9 (1)
200	161 (6)	9 (2)	58 (4)	11 (2)
220	176 (7)	10 (2)	56 (5)	17 (2)
240	215 (8)	19 (3)	60 (5)	13 (2)
298	258 (9)	25 (3)	84 (6)	17 (2)

largest principal amplitude is directed approximately perpendicular to the N—D bond and parallel to the basal plane; it increases rapidly with temperature and at room temperature the r.m.s. amplitude is 0.56 Å.

These results can be interpreted as either a shift in the equilibrium orientation of the ion together with a large increase in thermal motion, or as an attempt to accommodate, within a model based on a single deuterium site, two equilibrium positions with roughly equal populations, in which the N—D bonds point at respectively the axial and equatorial O atoms. The first interpretation would require a decrease of the ammonium ion librational frequency at temperatures above about 90 K, because the rapid increase in the thermal amplitude corresponding to libration about the c axis implies a considerable decrease in the force constant for this motion. In fact, no reduction in the ammonium ion librational frequency in NH_4ReO_4 is seen at 180 K, although the ammonium ion external modes are broad and weak at this temperature and disappear altogether

Table 6. *Structural data*

Bond distances are given in Å and angles in °.

T (K)	α	β	N—D	D—N—D	Re—O	O—Re—O
Series I						
20	18.92 (12)	31.67 (7)	1.025 (2)	108.9 (2)	1.733 (2)	110.9 (1)
40	18.75 (12)	31.62 (7)	1.025 (2)	108.7 (2)	1.733 (2)	110.8 (1)
60	18.80 (12)	31.58 (7)	1.024 (2)	108.7 (2)	1.733 (2)	110.9 (1)
80	18.77 (12)	31.50 (7)	1.024 (2)	108.9 (2)	1.733 (2)	110.8 (1)
100	18.72 (12)	31.39 (7)	1.021 (2)	108.7 (2)	1.732 (2)	110.9 (1)
120	18.32 (16)	31.14 (7)	1.021 (2)	108.8 (2)	1.734 (2)	110.6 (1)
140	17.57 (16)	31.04 (7)	1.015 (2)	109.3 (3)	1.732 (2)	110.4 (2)
Series II						
140	17.81 (12)	30.97 (6)	1.010 (1)	108.5 (2)	1.721 (2)	110.2 (1)
160	17.13 (13)	30.66 (7)	1.004 (2)	108.2 (2)	1.723 (2)	110.3 (1)
180	15.57 (17)	30.27 (7)	0.989 (2)	107.7 (2)	1.725 (2)	110.4 (1)
200	11.72 (26)	29.67 (9)	0.971 (2)	106.1 (3)	1.724 (2)	110.1 (2)
220	7.10 (40)	29.14 (10)	0.953 (3)	106.8 (3)	1.730 (2)	110.1 (2)
240	−1.50 (50)	28.36 (10)	0.936 (3)	105.0 (3)	1.732 (2)	109.9 (2)
298	−10.19 (74)	27.72 (11)	0.913 (4)	104.2 (5)	1.728 (2)	110.1 (2)

Table 7. *Cation–oxygen distances* (Å)

T (K)	N—O_{ax}	N—O_{eq}	D—O_{ax}	D—O_{eq}
Series I				
20	2.867 (2)	3.034 (2)	1.878 (2)	2.736 (3)
40	2.866 (2)	3.037 (2)	1.877 (2)	2.736 (3)
60	2.867 (2)	3.037 (2)	1.880 (2)	2.738 (3)
80	2.868 (2)	3.039 (2)	1.880 (2)	2.740 (3)
100	2.870 (2)	3.040 (2)	1.885 (2)	2.741 (3)
120	2.867 (2)	3.042 (2)	1.883 (2)	2.739 (3)
140	2.870 (2)	3.043 (2)	1.895 (3)	2.730 (3)
Series II				
140	2.871 (2)	3.046 (2)	1.987 (2)	2.737 (2)
160	2.872 (2)	3.040 (2)	1.906 (2)	2.724 (3)
180	2.874 (2)	3.028 (2)	1.926 (2)	2.697 (3)
200	2.876 (2)	3.020 (2)	1.951 (4)	2.643 (4)
220	2.875 (2)	3.008 (2)	1.984 (4)	2.579 (6)
240	2.872 (2)	3.008 (2)	2.025 (5)	2.486 (7)
298	2.890 (3)	3.003 (3)	2.107 (6)	2.402 (9)

near room temperature (Korppi-Tommola, Devarajan, Brown & Shurvell, 1978). Hence the second interpretation is to be preferred, and the present experiments provide strong support for the basic assumption of pseudo-spin theory, namely that there are two possible orientations of the ammonium ion, which differ in energy by an amount which depends on the unit-cell dimensions. Further refinements in the theory are required, however, since the data in Table 1 show that the assumption that the unit-cell volume is constant is not a good approximation.

An attempt was made to refine the room temperature data using a split D atom, in accordance with the pseudo-spin theory. The initial D-atom positions were based upon the equatorial and axial orientations of the ammonium ion, and the relative populations of the two sites were adjustable parameters. The refinement led to a low R value, but the two D-atom positions which resulted corresponded to unacceptable ND_4^+ ion geometry, and so the refinement was rejected.

This work was supported by the Natural Sciences and Engineering Research Council of Canada. Helpful discussions with Professor D. R. Taylor are gratefully acknowledged.

References

BROWN, R. J. C., POWELL, B. M. & STUART, S. N. (1993). *Acta Cryst.* C**49**, 214–216.
BROWN, R. J. C., SEGEL, S. L. & DOLLING, G. (1980). *Acta Cryst.* B**36**, 2195–2198.
BROWN, R. J. C., SHORTREED, M. E., SZABO, A. J., POWELL, B. M. & STUART, S. N. (1992). *Z. Naturforsch. Teil A*, **47**, 308–312.
BROWN, R. J. C., SMELTZER, J. G. & HEYDING, R. D. (1976). *J. Magn. Reson.* **24**, 269–274.
FIGGIS, B. N., KUCHARSKI, E. S. & FORSYTH, J. B. (1991). *Acta Cryst.* C**47**, 419–412.
HEWAT, A. W. (1979). *Acta Cryst.* A**35**, 248.
KORPPI-TOMMOLA, J., DEVARAJAN, V., BROWN, R. J. C. & SHURVELL, H. F. (1978). *J. Raman Spectrosc.* **7**, 96–100.
KRUGER, G. J. & REYNHARDT, E. C. (1978). *Acta Cryst.* B**34**, 259–261.
LOCK, C. J. L. & TURNER, G. (1975). *Acta Cryst.* B**31**, 1764–1765.
SEARS, V. F. (1986). *Methods of Experimental Physics*, Vol. 23A, edited by K. SKÖLD & D. L. PRICE, pp. 521–550. San Diego: Academic Press.
SEGEL, S. L., KARLSSON, H., GUSTAVSON, T. & EDSTROM, K. (1985). *J. Chem. Phys.* **82**, 1611–1612.
TAYLOR, D. R. (1987). *J. Chem. Phys.* **87**, 773–774.
TAYLOR, D. R. (1989). *Phys. Rev. B.* **40**, 493–499.
WILES, D. B. & YOUNG, R. A. (1981). *J. Appl. Cryst.* **14**, 149–151.

Acta Cryst. (1993). B**49**, 468–474

Structure of RNi$_3$Al$_9$ (R = Y, Gd, Dy, Er) with Either Ordered or Partly Disordered Arrangement of Al-Atom Triangles and Rare-Earth-Metal Atoms

BY R. E. GLADYSHEVSKII, K. CENZUAL, H. D. FLACK AND E. PARTHÉ

Laboratoire de Cristallographie, Université de Genève, 24 quai Ernest-Ansermet, CH-1211 Geneva 4, Switzerland

(*Received* 16 *December* 1991; *accepted* 4 *November* 1992)

Abstract

ErNi$_3$Al$_9$, M_r = 586.22, trigonal, new type, $hR78$, $R32$ – f^2edc^4 (No. 155), a = 7.2716 (5), c = 27.346 (3) Å, V = 1252.2 (2) Å^3, Z = 6, D_x = 4.664 Mg m^{-3}, λ(Mo $K\alpha$) = 0.71073 Å, μ = 17.654 mm^{-1}, $F(000)$ = 1614, T = 293 K, wR = 0.021 for 785 contributing unique reflections. The structure is built up of three kinds of monoatomic layer perpendicular to **c**: Al-atom layers with triangular mesh, Ni-atom layers with triangular mesh and layers containing two rare-earth-metal atoms for one Al-atom triangle. GdNi$_3$Al$_9$ [a = 7.3006 (9), c = 27.478 (5) Å, wR = 0.020 for 791 reflections] is isotypic. YNi$_3$Al$_9$ [a = 7.2894 (7), c = 27.430 (5) Å, wR = 0.035 for 635 reflections] and DyNi$_3$Al$_9$ [a = 7.2723 (9), c = 27.344 (6) Å, wR = 0.027 for 682 reflections] crystallize in related structures with a partly disordered arrangement of Al-atom triangles and rare-earth-metal atoms. Similar monoatomic layers to those in ErNi$_3$Al$_9$ build up the orthorhombic structure of $Y_2Co_3Al_9$ ($Y_2Co_3Ga_9$ type). The stoichiometry 1:3:9 is related to that of $R_2T_3Al_9$ by replacing every second mixed layer of composition R_2Al_3 by an Al-atom layer (Al_3): $6RT_3Al_9 = 6R_2T_3Al_9 - 3R_2Al_3 + 3Al_3$.

Introduction

The Al-rich part of the rare-earth–transition metal–Al phase diagrams appears to be very complicated, with a large number of compounds of very similar composition. In the Y–Ni–Al system, for example, five compounds containing more than 50 at.% Al, have been identified (Rykhal' & Zarechnyuk, 1977; Gladyshevskii & Parthé, 1992). We report here the structures of four new rare-earth-metal–Ni aluminides, two of which are isotypic whereas the other two crystallize in partly disordered, closely related structures.

Experimental

Samples were prepared from high-purity elements (Y, Gd, Dy, Er ≥ 99.9%, Ni and Al ≥ 99.999%) by arc melting under argon atmosphere and annealed at 1073 K for two weeks in a silica tube under an argon atmosphere (400 mm Hg). Single crystals were mounted on a Philips PW1100 automatic four-circle diffractometer, Mo $K\alpha$ radiation with graphite monochromator, ω–2θ scan mode. An absorption correction was made using *LSABS* (Blanc, Schwarzenbach & Flack, 1991), the anomalous-dispersion coefficients were taken from *International Tables for X-ray Crystallography* (1974, Vol. IV). Systematic absences led to the following possible space groups: $R3$, $R\bar{3}$, $R32$, $R3m$ and $R\bar{3}m$ (*International Tables for Crystallography*, 1983, Vol. A). The structure of ErNi$_3$Al$_9$ was solved in space group $R32$ by *MULTAN*87 (Debaerdemaeker, Germain, Main, Tate & Woolfson, 1987); one rare-earth-metal,

0108-7681/93/030468-07$06.00